Electronic distributions and pseudo-gap in quasicrystalline decagonal $Al_{65}Cu_{15}Co_{20}$ and $Al_{70}Co_{15}Ni_{15}$ alloys

1996 J. Phys.: Condens. Matter 8 6213

(http://iopscience.iop.org/0953-8984/8/34/011)

J. Phys.: Condens. Matter **8** (1996) 6213–6228. Printed in the UK

Electronic distributions and pseudo-gap in quasicrystalline decagonal $Al_{65}Cu_{15}Co_{20}$ and $Al_{70}Co_{15}Ni_{15}$ alloys

Esther Belin-Ferré†, Zoltán Dankházi†‡, Vincent Fournée†, Anne Sadoc§‖, Claire Berger¶, Herbert Müller+ and Hans Kirchmayr+

† Laboratoire de Chimie Physique Matière et Rayonnement, Unité de Recherche associée au CNRS 176, and Groupement de Recherche Concertation et Investigation des Quasicristaux, 11 rue Pierre et Marie Curie, 75231 Paris Cédex 05, France

‡ Institute for Solid State Physics, Muzéum krt 6–8, 1088 Budapest, Hungary

§ Laboratoire pour l'Utilisation du Rayonnement Electromagnétique, CNRS, MENESR, IP, Commissariat à l'Energie Atomique and Groupement de Recherche Concertation et Investigation des Quasicristaux, Université Paris-Sud, 91405 Orsay Cédex, France

‖ LPMS, 49 avenue des Genottes. BP 8428, 95806 Cergy-Pontoise Cédex, France

¶ Laboratoire d'Etudes des Propriétés Electroniques des Solides, CNRS and Groupement de Recherche Concertation et Investigation des Quasicristaux, 25 Avenue des Martrys. BP 166 X, 38042 Grenoble Cédex, France

+ Institut für Experimentalphysik, Technical University Vienna, Wiedner Hauptstrasse 8–10, A-1040 Wien, Austria

Received 5 February 1996, in final form 26 April 1996

Abstract. Electronic state distributions of decagonal $Al_{65}Cu_{15}Co_{20}$ and $Al_{70}Co_{15}Ni_{15}$ quasicrystals have been investigated by experimental means using the soft-x-ray spectroscopy technique complemented by photoemission spectroscopy measurements. In both quasicrystals, interaction is shown within an energy range of 2 eV below the Fermi level between the Al states and either the Co 3d states or both the Ni 3d and the Co 3d states. In $Al_{65}Cu_{15}Co_{20}$, the Cu 3d states are observed in the middle of the occupied band. The formation of a significant pseudo-gap at the Fermi level is shown in the Al 3p and 3s–d distributions of these alloys. The comparison with available photoemission data an $Al_{65}Cu_{20}Co_{15}$ and $Al_{70}Co_{15}Ni_{15}$ samples shows good agreement in the energy positions of Cu, Co and Ni occupied states. The results for $Al_{65}Cu_{15}Co_{20}$ are compared with calculations of densities of states for two models of the Al–Co–Cu decagonal quasicrystals. Very good agreement between experiment and one of these calculations is found for the Al distributions. For $Al_{70}Co_{15}Ni_{15}$, fair agreement between the present results and data for crystalline Al_5Co_2 is shown. The Al p and Ni s–d unoccupied states are considered as well in $Al_{70}Co_{15}Ni_{15}$. It is suggested that a slight charge transfer may occur from Al to Ni in this sample and that most of the Al p unoccupied states presumably occur from the contribution of the quasiperiodic planes in this specimen.

1. Introduction

Soon after icosahedral quasicrystalline alloys were found by Shechtman *et al* (1984), decagonal phases (sometimes referred to as T phases) were recognized by Bendersky (1985) in the Al–Mn system. These phases combine two structural characteristics since they possess quasiperiodic planes with a tenfold rotational symmetry axis that are perpendicular to one axis of crystalline-like periodicity. The first alloys of this new class of quasicrystals (Bendersky 1985) were metastable. Later, stable decagonal quasicrystals were found in the Al–Co–Cu system (He *et al* 1988) which gave impetus to the analysis of their atomic

0953-8984/96/346213+16$19.50

arrangement (Tsai *et al* 1989, Liao *et al* 1992, Steurer 1993, 1994, Steurer *et al* 1993, Fettweiss *et al* 1994, Wittmann *et al* 1995) as well as to the study of their properties and electronic structure (Gozlan 1991, Stadnik *et al* 1995a, b). In the case of icosahedral quasicrystals, many of the electronic properties have been inferred from the existence of a more or less marked pseudo-gap at the Fermi level E_F in the densities of states (DOS) (see, e.g., Poon (1992) and Berger *et al* (1993), and references therein). The decagonal Al–Co–Cu and Al–Co–Ni quasicrystal structures are isotopic. They are built up of two quasiperiodic atomic layers with a stacking sequence and a translation period of about 4 Å. Columnar clusters of about 20 Å diameter are parallel to the local tenfold screw axes; they are formed by ten pentagonal antiprismatic columns surrounding a central column; these clusters are found to be the basic structural building elements. Quasiperiodicity is forced by the formation of interconnected networks of closed icosagonal rings of pentagonal and rectangular structure motifs and columnar clusters. The global structure acts as a weak matching rule that stabilizes the quasiperiodic structure (Steurer 1993, 1994, Steurer *et al* 1993). The specificity of the electronic properties of these decagonal quasicrystals is connected to their structural anisotropy; for example the electric conductivity at low temperatures is non-metallic like in the quasicrystalline plane and metallic like along the periodic axis. A calculation by Trambly de Laissardière and Fujiwara (1994a, b) made for a model Al–Cu–Co alloy predicts that a pseudo-gap should exist at E_F in the DOS whereas such a pseudo-gap is not pointed out in another calculation by Sabiryanov *et al* (1995) for a similar alloy with different nominal composition. Furthermore, Stadnik *et al* (1995a, b) have investigated through photoemission means the valence bands of $Al_{65}Cu_{20}Co_{15}$ and $Al_{70}Co_{15}Ni_{15}$ decagonal quasicrystals and they claim that no pseudo-gap exists in these phases.

Thus, more insight is needed into the electronic structure of decagonal phases and related crystalline approximants. One possibility for studying the distributions of occupied band (OB) and unoccupied band (UB) states is to combine both soft-x-ray spectroscopy (SXS) and x-ray photoemission spectroscopy (XPS) techniques. These have already been used to investigate OBs and UBs in icosahedral Al–Cu (or Pd)-transition-metal (TM) or Al–TM quasicrystals (Belin and Traverse 1991, Belin *et al* 1992, 1994a, b, 1995, Belin and Dankházi 1993, Sadoc *et al* 1993). For the OBs, the results differ according to the chemical composition of the sample. They can be summarized as follows. In Al–Cu (or Pd)–TM alloys, interaction exists at E_F between hybridized Al p–d and TM d states; the Al states exhibit a pseudo-gap at this energy and a depletion in the middle of the band coincides with the maximum of the Cu (or Pd) occupied d-like subband. For Al–TM alloys, interaction at E_F between hybridized Al p–d and TM d states is preserved; the pseudo-gap is still present but no depletion is seen in the middle of the OBs.

In this paper, we report an experimental investigation of two single-phase decagonal quasicrystalline $Al_{65}Cu_{15}Co_{20}$ and $Al_{70}Co_{15}Ni_{15}$ alloys whose atomic structures are analogous although the chemical order should not be the same in both phases (Steurer 1993, 1994, Steurer *et al* 1993). The paper is divided as follows. In section 2, the principles of SXS and XPS are summarized; information about the sample preparation and characterization including experimental procedures is also given. The results are presented in section 3. In section 4, the results are briefly compared with those of the pure elements and with crystalline approximants. They are discussed in connection with the XPS data from Stadnik *et al* (1995a, b) on $Al_{65}Cu_{20}Co_{15}$ and $Al_{70}Co_{15}Ni_{15}$ and with DOS calculations for a model decagonal Al–Cu–Co phase by Trambly de Laissardière and Fujiwara (1994a, b) and by Sabiryanov *et al* (1995). For $Al_{70}Co_{15}Ni_{15}$, comparison is made with calculations for crystalline Al_5Co_2 which is an approximant of decagonal quasicrystals (Song and Ryba 1992). Finally, the results are summarized in the conclusion.

2. Experiments

2.1. Principles

The soft-x-ray emission spectroscopy (SXES) and soft-x-ray absorption spectroscopy (SXAS) techniques investigate separately OB and/or UB states of the various components of a solid due to transitions that involve an inner level $\mathcal{L}_{n,l}$ and either the OB or UB states. The x-ray transitions are governed by dipole selection rules ($\Delta l = \pm 1$ and $\Delta \mathrm{j} = 0, \pm 1$) and the inner hole is on a given atomic site of the solid. This makes SXS both a symmetry- and a site-selective technique. The energy distributions of the intensities emitted or absorbed during SXES or SXAS processes are proportional to $|\mathrm{M}|^2 N(\varepsilon)\mathcal{L}_{n,l}$. M is the matrix element of the transition probability that depends upon the overlap between the initial and final wavefunctions of the system and it may be considered as being constant over the energy ranges which are investigated here. $N(\varepsilon)$ is the OB or UB DOS probed during the measurement. $\mathcal{L}_{n,l}$ is the Lorentzian-like energy distribution of the inner level involved in the x-ray transition. Although no absolute DOS values are obtained from these techniques, the shapes of the emission or absorption spectral curves are directly connected to either the occupied or the unoccupied partial DOSs spatially averaged over the bulk material.

In the XPS technique, electrons are ejected from the solid owing to the interaction with an incident radiation. According to the energy of the incident photons, the electrons are ejected from the very surface of the solid up to a thickness of sample of a few nanometres. The kinetic energies of the outcoming electrons are measured; consequently the corresponding binding energies are gained provided that suitable calibration is made to account for the work function of the solid. The binding energies of the inner levels are obtained separately. On the contrary, the binding energies of the electrons of the OB are achieved all together. Note that, owing to photoemission cross sections that considerably favour d and f states (Yeh 1993), this technique does not provide any view of the energy distributions of s and p OB states in alloys containing both sp metals and TM or rare earths. This emphasizes the interest of using the SXS technique to analyse the electronic distributions of Al in quasicrystalline alloys since it is a major component in these intermetallics and since one can expect that s and p states which are extended states could be much more sensitive than localized states to any kind of modification of the atomic environment.

The binding energies of the core levels involved in the various x-ray transitions which we investigate can be measured with respect to the Fermi level energy $\mathrm{E_F}$ through XPS experiments owing to proper calibration of the binding energy scale. Consequently, $\mathrm{E_F}$ may be set on the corresponding x-ray transition energy scales. This allows adjustment of the partial local occupied and/or unoccupied electronic distributions in the same absolute energy scale. So, combining SXS and XPS techniques makes it possible to obtain a picture of the OBs and UBs and to gain insight into the electronic interactions in the solid.

2.2. The samples

Ingots of $Al_{65}Cu_{15}Co_{20}$ and $Al_{70}Co_{15}Ni_{15}$ were first arc melted in an argon atmosphere, from pure (99.99%) elemental constituents. Thin ribbons of the order of 35–50 μm thick were then melt spun in a He atmosphere. Annealing of samples was achieved in high vacuum at 900 °C and 920 °C for 48 h and then prompt cooling for $Al_{65}Cu_{15}Co_{20}$ and $Al_{70}Co_{15}Ni_{15}$, respectively. The samples were characterized by powder x-ray diffraction using the Cu Kα line. The spectra could be indexed within the planar T-phase indexation scheme (Takeuchi

and Kimura 1987), with five vectors in the quasicrystalline planes and one vector along the periodic axis. This indexation scheme is best adapted to a periodic stacking of planes describing the T-phase structure (McRae *et al* 1990). The positions and peak intensities in our diagrams were in good agreement with results published elsewhere (Tsai *et al* 1989). The width peaks measured for our samples reveal a good structural quality.

2.3. Experimental procedures

To describe the energy distribution of OB and UB states we hve measured several x-ray transitions, as shown in table 1. The soft-x-ray emission spectra were obtained using vacuum spectrometers fixed with bent SiO_2 $10\bar{1}0$ or RbAP crystals or a grating of energy resolutions ranging from ± 0.3 (SiO_2 $10\bar{1}0$ and grating) to ± 0.5 eV (RbAP). The spectra were excited with incoming electrons or photons. The samples were water cooled. The emitted photons were collected with gas flow proportional counters or a photocathode coupled together with a channeltron. The Al K and Ni L_{III} absorption edges were scanned at the synchrotron radiation facility of the Laboratoire pour l'Utilisation du Rayonnement Electromagnétique (LURE), Orsay, France. The yield technique was used at the Super ACO storage ring (experimental station SA 32) owing to two-crystal monochromators equipped with SiO_2 $10\bar{1}0$ slabs for the study of the Al K edge and beryl $10\bar{1}0$ crystals for investigating the Ni L_{III} edge. The energy resolutions were the same as for SXES measurements. Soft-x-ray spectra of pure Al, Cu, Co and Ni metals were also measured for comparison and energy calibration purposes.

Table 1. Analysed x-ray transitions, states investigated, energy ranges studied, experimental techniques and widths of the inner level involved in the x-ray transition. The values of the widths of inner levels are taken from Krause and Oliver (1979).

X-ray transition	States investigated	Energy range (eV)	Technique	Width of the inner level (eV)
Al Kβ : OB $\rightarrow$ 1s	Al 3p	1550–1565	SXES	0.40
Al $L_{2.3}$: OB $2p_{3/2}$	Al 3s–d	55–75	SXES	$<$ 0.1
Cu Lα : OB $\rightarrow$ $2p_{3/2}$	Cu 3s–d	920–940	SXES	0.56
Co Lα : OB $\rightarrow$ $2p_{3/2}$	Co 3s–d	770–785	SXES	0.43
Ni Lα : OB $\rightarrow$ $2p_{3/2}$	Ni 3s–d	840–860	SXES	0.48
Al K : 1s $\rightarrow$ UB	Al p	1555–1585	SXAS	0.40
N L_{III} : $2p_{3/2}$ $\rightarrow$ UB	Ni s–d	850–880	SXAS	0.48

In addition to the instrumental resolutions of the different spectrometers, it is necessary to account for the intrinsic broadening by the inner levels involved in the x-ray transitions that is inherent to the SXS technique (see table 1). Thus, finally, the experimental energy resolutions are less than 0.5 eV in the case of the Al spectra and within 0.6–0.8 eV for the spectra of the other elements. Note that the resolution of XPS experiments is generally about 0.4 eV, i.e. similar to that obtained in the SXS measurements of Al spectra.

3. Results

The Al, Cu, Co and Ni $2p_{3/2}$ binding energies were obtained from XPS measurements using the Mg or Al Kα radiations (Mg or Al $2p_{3/2}$ $\rightarrow$ 1s) which ensures the contribution of the bulk material. The binding energy scale was calibrated with respect to the C 1s level taken

equal to 285.0 eV. The binding energy of the Al 1s level that could not be reached directly was deduced from the energy of the Al $2p_{3/2}$ level complemented by the measurement of the energy of the Al Kα ($2p_{3/2} \rightarrow 1s$) emission line. Compared with pure metals, the levels in both quasicrystals were found to be shifted by 0.4 ± 0.1 eV for Al, 0.8 ± 0.3 eV for Cu, 0.7 ± 0.3 eV for Co and 0.3 ± 0.3 eV for Ni. In the case of the $Al_{65}Cu_{15}Co_{20}$ sample, we did not obtain sufficient accuracy in measuring the binding energy of the Co $2p_{3/2}$ level; thus we used our value for Co in $Al_{70}Co_{15}Ni_{15}$ to adjust the Co Lα distribution curve of $Al_{65}Cu_{15}Co_{20}$ on the binding energy scale; note that in this way, within the experimental accuracy, we found that the maximum of the Co 3d state distribution is at the same energy position as measured using the XPS technique by Stadnik *et al* (1995a, b) for $Al_{65}Cu_{20}Co_{15}$. Finally, we could place E_F on the various x-ray transition energy scales within ± 0.1 eV for Al and not better than ± 0.3 eV for the other elements.

The SXS emission curves are normalized on the intensity scale between their own maximum and the baseline taken in energy ranges where the variation in intensity is negligible. The absorption curves are normalized as well. In the figure describing both the Al 3p and the Al p state distributions, the absorption curve is adjusted to the same intensity at E_F as that of the corresponding emission curve.

Figures 1(a) and 1(b) show the Al 3p and 3s–d distribution curves for $Al_{65}Cu_{15}Co_{20}$ and $Al_{70}Co_{15}Ni_{15}$, respectively, as well as for pure FCC Al (insert in figure 1(a)).

The curves for pure Al display an abrupt emission edge. The arctangent-like emission edge of the Al 3p curve cuts E_F at half the maximum intensity. Beyond the edge, there is a rounded maximum at about 1.3 eV and a parabolic-like decrease in intensity that is continued by a long monotonical decreasing tail. The edge of the Al 3s–d curve is followed by a sharp intense peak almost at E_F and then the shape is parabolic.

For the two decagonal quasicrystalline alloys, the shapes of the Al 3p as well as Al 3s–d curves differ somewhat from those for pure Al in that they show emission edges much less steep than in the metal.

For $Al_{65}Cu_{15}Co_{20}$, the maximum of the Al 3p curve is shifted to $E_F + 2.5 \pm 0.1$ eV. Both sides of the maximum are structured as seen from the slight feature a at about $E_F + 1.3$ eV and the shoulder after the relative plain b at about $E_F + 4.3$ eV. The Al 3s–d curve shows two distinct well separated broad peaks of nearly same intensity with a pronounced minimum β in between at around 4.0 eV below E_F. The maximum of the first broad peak is at $E_F + 2.5 \pm 0.1$ eV. In the energy range of feature a of the Al 3p curve there is a change in slope denoted α just after the Al 3s–d edge. The second maximum γ at $E_F + 6.2 \pm 0.2$ eV and feature δ at $E_F + 8 \pm 0.2$ eV are in energy ranges where the intensity of the Al 3p curve strongly decreases with increasing binding energy. The general shapes of the Al curves are similar to those already observed for crystalline or quasicrystalline Al-based alloys containing Cu. Indeed, as recalled above, a depletion is shown in the middle of the Al 3s–d distribution curve whereas a shoulder is seen in the same energy range of the Al 3p curve (Fuggle *et al* 1977, Belin and Dankházi 1993, Belin *et al* 1994a, b, 1995, Nakamura and Mizutani 1994, Trambly de Laissardière and Fujiwara 1994a, b).

In $Al_{70}Co_{15}Ni_{15}$, as in other Al–TM alloys (Belin and Traverse 1991, Belin *et al* 1992, Dankházi *et al* 1993) the Al 3p curve turns out to have a sharp broad peak. Here, maximum c is 3 eV below E_F and the emission edge exhibits two shoulders a and b at $E_F + 0.9 \pm 0.1$ eV and $E_F + 1.6 \pm 0.1$ eV, respectively. The intensity of the high-binding-energy side of the curve decreases monotonically; however, a faint smooth broad bump d is present at about 5.4 eV below E_F. From E_F towards increasing energies, the edge of the Al 3s–d curve is followed by firstly a slight hump α that coincides within experimental accuracy with feature a of the Al 3p curve, secondly two marked minima β and γ that are in the energy ranges

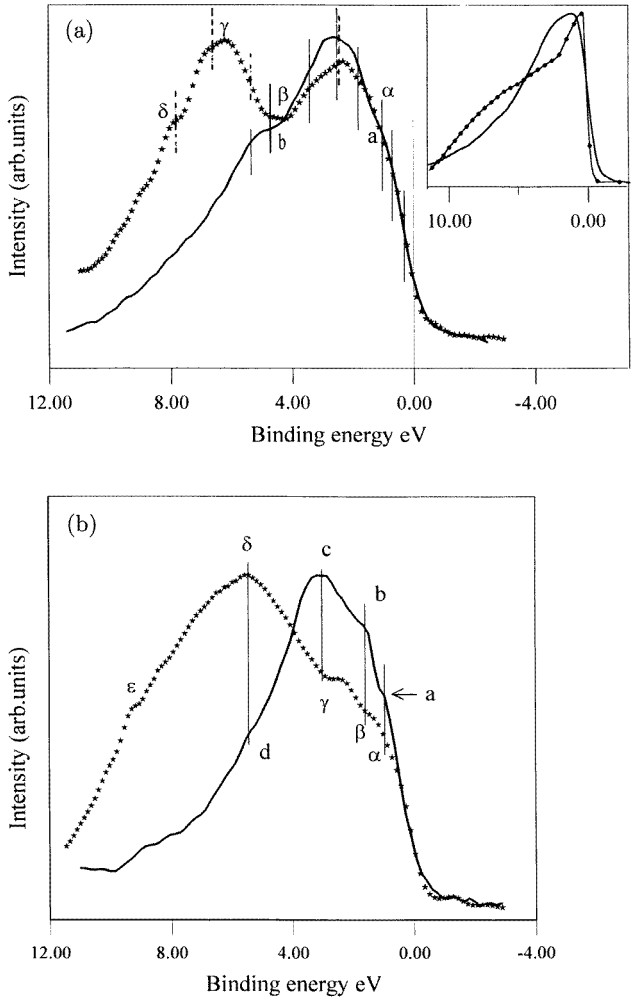

Figure 1. (a) Al 3p (——) and Al 3s–d (⋆) distribution curves in $Al_{65}Cu_{15}Co_{20}$. For the significance of the broken and full vertical lines, see text. The inset shows Al 3p (——) and Al 3s–d (——●——) distribution curves for pure FCC Al. (b) Al 3p (——) and Al 3s–d (⋆) distribution curves for $Al_{70}Co_{15}Ni_{15}$. The vertical lines are a guide for the eyes.

of feature b and maximum c of the Al 3p curve, thirdly a broad maximum δ that is in the energy range of feature d of the Al 3p curve and fourthly a shoulder ε. The vertical lines in figure 1(b) are simply a guide for the eyes to demonstrate the coincidence between the features of the Al 3s–d and Al 3p distribution curves.

Let us emphasize that for both $Al_{65}Cu_{15}Co_{20}$ and $Al_{70}Co_{15}Ni_{15}$ quasicrystals the intensities of the Al 3p and 3s–d curves at E_F are much lower than for pure Al. The emission edges are pushed away from E_F so that they cut the Fermi level at a lower intensity than half the maximum intensity as for pure Al. We shall return to this point in the next section.

The shapes of the Cu, Co or Ni 3d–4s curves do not differ significantly from those of the pure metals as shown in figures 2, 3 and 4, respectively. Note that these curves

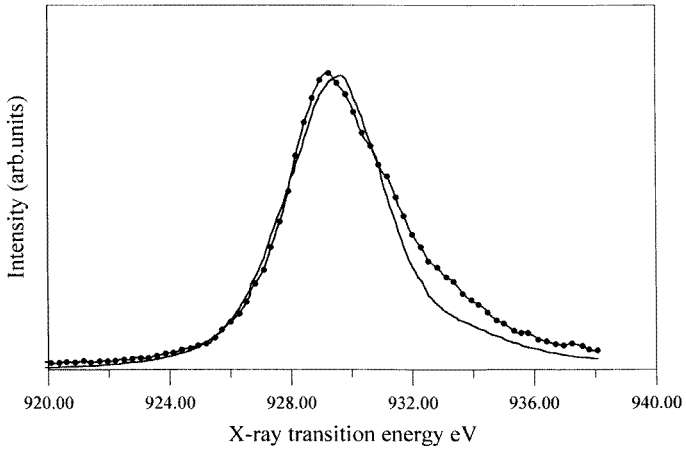

Figure 2. Cu 3d–s distribution curves for $Al_{65}Cu_{15}Co_{20}$. (—●—) and for pure Cu (——).

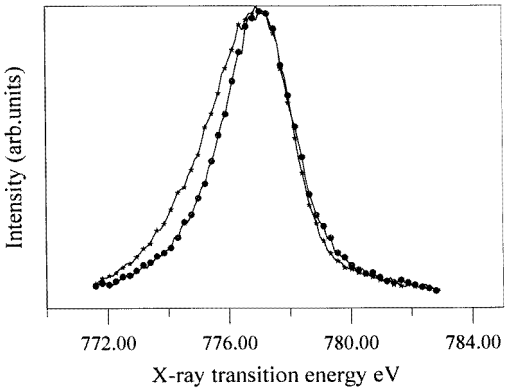

Figure 3. Co 3d–s distribution curves for $Al_{65}Cu_{15}Co_{20}$. (—●—) and for pure Co (—★—).

mainly reflect the distribution of 3d states since x-ray transition probabilities favour p → d transitions over p → s transitions. When going from metal to alloys, the Co and Ni 3d curves are shifted slightly to higher x-ray transition energies, whereas the Cu 3d curve is shifted towards low x-ray transition energies. The full widths at half-maximum intensity of the peak are reduced by about 1 eV for Co 3d and are the same within the limits of the experimental accuracy for Ni 3d and Cu 3d. The energy distances E_F–maxima of the Cu and TM distributions in $Al_{65}Cu_{15}Co_{20}$ are 3.9 ± 0.1 eV and 0.8 ± 0.1 eV for Cu 3d and Co 3d, respectively, whereas in $Al_{70}Co_{15}Ni_{15}$ they are 1.3 ± 0.1 eV and 0.8 ± 0.1 eV for Ni 3d and Co 3d, respectively.

Adjustment of all the occupied distributions are displayed for $Al_{65}Cu_{15}Co_{20}$ in figure 5 and for $Al_{70}Co_{15}Ni_{15}$ in figure 6. This shows that, in $Al_{65}Cu_{15}Co_{20}$, the OB picture is analogous to that already observed in ternary or quaternary crystalline or quasicrystalline alloys containing both Cu and a TM. Indeed in such alloys, as mentioned above, one finds that TM 3d (4d or 5d) states are near E_F, Cu 3d states are in the middle of the band and

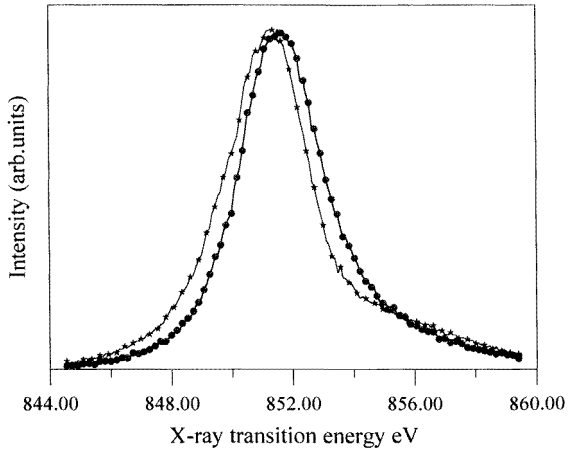

Figure 4. Ni 3d–s distribution curves for $Al_{70}Co_{15}Ni_{15}$. (—●—) and for pure Ni (—★—).

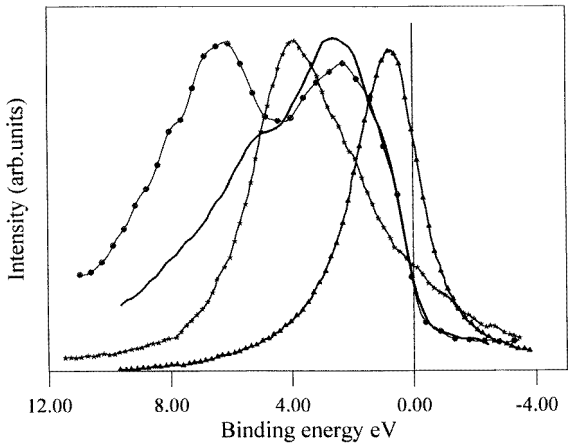

Figure 5. Occupied distribution curves for $Al_{65}Cu_{15}Co_{20}$: ——, Al 3p; —●—, Al 3s–d; —★—, Cu 3d; —●—, Ni 3d.

the Al subbands are split into two subbands located on each side of the Cu 3d states curve (Belin and Dankhazi 1993, Belin *et al* 1992, 1994a, b). In spite of this, the OB picture for $Al_{70}Co_{15}Ni_{15}$ resembles that obtained for binary Al–TM alloys; TM 3d states are present close to E_F and the Al states are spread over an energy range of about 10 ev below E_F (Belin and Traverse 1991, Belin *et al* 1991, Traverse *et al* 1996).

Figure 7 shows the unoccupied Ni d states in pure metal and in decagonal $Al_{70}Co_{15}Ni_{15}$. In the metal the curve exhibits a sharp peak A (the so-called 'white line') followed towards decreasing binding energy by two broad faint bumps B and C. In the alloy, the white line is no longer present; a very broad peak β is approximately at the same energy as feature B in the metal. This broad peak is continued by a monotonic decrease in intensity towards the energy range of structure C of the spectrum of pure Ni.

Figure 8 displays the Al p curves for pure Al and for $Al_{70}Co_{15}Ni_{15}$. In the metal the curve presents an abrupt absorption edge that is followed by a monotonic increase in

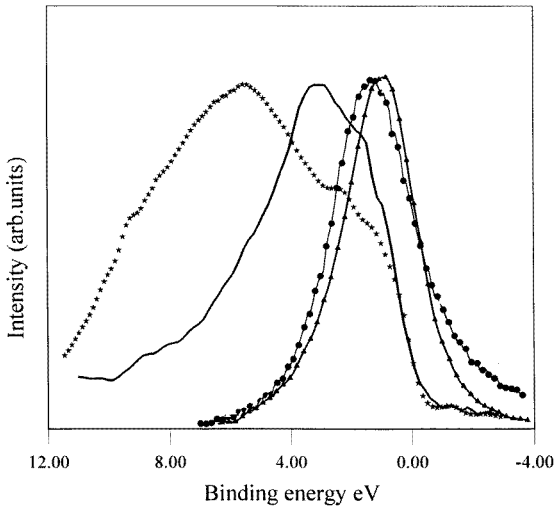

Figure 6. Occupied distribution curves for $Al_{70}Co_{15}Ni_{15}$: ——, Al 3p; —★—, Al 3s–d; —●—, Ni 3d; —▲—, Co 3d.

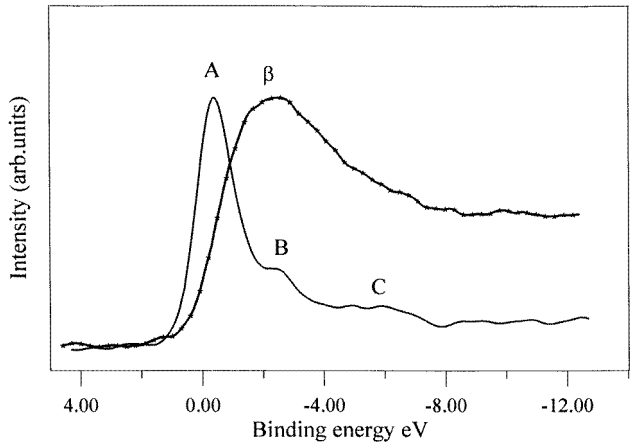

Figure 7. Ni d–s distribution curves for $Al_{70}Co_{15}Ni_{15}$: ——, pure Ni; —★—, Ni in $Al_{70}Co_{15}Ni_{15}$.

intensity up to about 7 eV from the edge where the curve shows a maximum. In the alloy, the edge is less steep and much less contrasted than in the metal; beyond the edge, the increase in intensity is also monotonic up to a flat maximum.

4. Discussion

Let us first discuss the OB state distributions. For pure Al, we have already mentioned that the Al 3p and 3s–d curves totally overlap and so the Al states are p–s hybridized over the whole OB with some p–s, d contribution near E_F. Indeed, the sharp peak observed in the Al 3s, d curve in the close vicinity of E_F is due to both the presence of a few d-like states

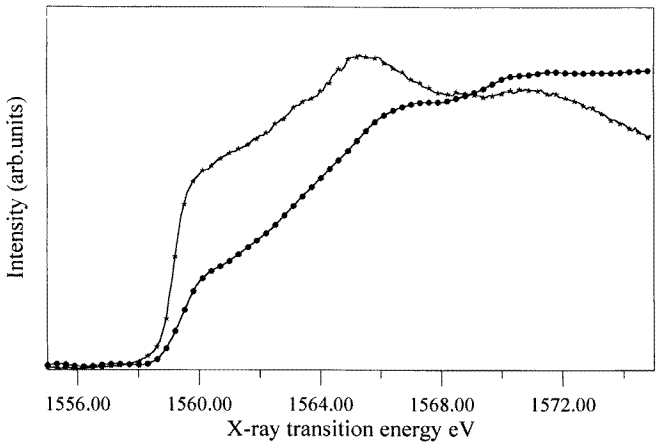

Figure 8. Al p distribution curves for $Al_{70}Co_{15}Ni_{15}$: ——★——, Al; ——●——, Al in $Al_{70}Co_{15}Ni_{15}$.

(Léonard 1978, Papaconstantopoulos 1986) and the well known Nozières–de Dominicis (1969) many-body effect. Such a peak is characteristic of a free-electron-like metal.

For $Al_{65}Cu_{15}Co_{20}$ and $Al_{70}Co_{15}Ni_{15}$ quasicrystals, over an energy range of about 4–5 eV from the Fermi level, the Al 3p and 3s–d curves are of significant intensity and totally overlap. Accordingly, the corresponding states are hybridized states as well. In the highly bonded part of the curves, the intensity of the Al 3p states seriously decreases whereas the Al 3s, d are dominant. Changes in the electronic distributions against energy are seen as dramatic changes in the shapes of the Al 3p and 3s–d curves for these alloys compared with the pure metal which emphasizes that the free-electron model does not apply in the interpretation of the electronic properties of the two quasicrystals. Let us recall here that the experimental results provide information averaged over the bulk material. Since, to our knowledge, no data are available concerning the actual positions of all the atoms in both Al–Cu–Co and Al–Co–Ni quasicrystals, we are not able to discuss possible differences in local environments. To analyse the results in more depth we shall compare in the following our data, with theoretical DOSs based on model alloys.

In the framework of the linear muffin-tin orbital (LMTO) method within the atomic sphere approximation (ASA), Trambly de Laissardière and Fujiwara (1994a, b) have calculated the band structure of a crystalline approximant $Al_{60}Cu_{27.3}Co_{12.7}$ of the quasicrystalline structure based on the cluster model proposed by Burkov (1991, 1992) for decagonal Al–TM alloys. Although the nominal concentrations in the model differ from experiment, let us compare the partial calculated DOSs and the experimental electronic distributions.

To begin with we shall discuss the Al states. The calculated Al s, p and d DOS curves are displayed in figure 9 (which is from the work of Trambly de Laissardière and Fujiwara (1994a, b). E_F is shown by a vertical axis with respect to the origin of the energy scale given in rydbergs and is taken as the origin of the binding energy scale. All the curves show a spiky structure especially in the regions of maximum DOSs. The occupied Al s DOSs are of very low intensity beyond about 2 eV from E_F and of high intensity beyond 5 eV from E_F. On the contrary, the intensity of the occupied Al d DOSs is very faint in the energy region beyond 5 eV from E_F and thus the Al states in this part of the OB are

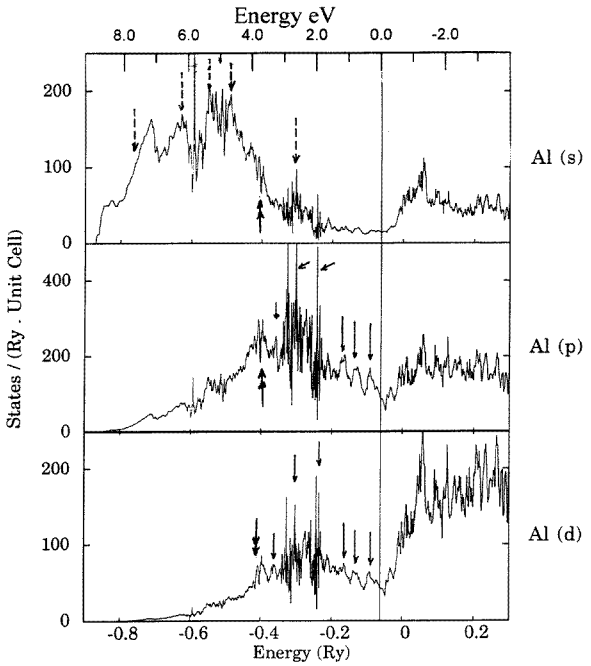

Figure 9. Calculated partial DOSs for $Al_{60}Cu_{27.3}Co_{12.7}$, a model crystalline approximant of the Al–Cu–Co decagonal quasicrystalline alloys. (Courtesy of G Trambly de Laissardière and T Fujiwara.)

almost pure s like in character. This confirms that states corresponding to the part of the Al 3s, d experimental curve that extend beyond feature β of figure 1(a) and mainly s like in character whereas the states in between feature β and E_F are more d like. The part of the Al d calculated curve between E_F and about 5 eV from E_F overlaps the Al p curve and the most salient features of both curves coincide in energy. Accordingly, p–d hybridization is very important since there is only a very faint s contribution in this energy range. This corresponds to the parts of the experimental Al 3p and Al 3s, d curves that are between E_F and features b and β of figure 1(a). The most important features of the partial calculated curves are shown by arrows in figure 9 to which the vertical lines in figure 1(a) correspond. The broken vertical lines denote s-like states whereas the thin full vertical lines indicate p–d states with a faint s-like contribution. Note that the states present at the Al 3p or 3s, d edges are essentially p–d-like states.

We have mentioned above that, in $Al_{65}Cu_{15}Co_{20}$, interaction exists between Al and Cu states in the middle of the OB and between Al and Co states in the vicinity of E_F, the result of which produces the splitting of the Al subbands in the energy range 4.3 eV below E_F and the shift back of the Al subband edges with respect to the pure metal near E_F. The splitting around 4.3 eV is indicated on the calculated curves of figure 9 by double arrows. The experimental Al edges are away from E_F in contrast with pure Al. The intensities of both Al 3p and Al 3s, d curves are much lower than for pure Al; whereas it is 50% of the maximum intensity in the pure metal it is reduced to about 20% of the maximum intensity in $Al_{65}Cu_{15}Co_{20}$. However, whereas the Al 3p edge cuts the Fermi level at half the maximum intensity in the pure metal, the same point in $Al_{65}Cu_{15}Co_{20}$ is distant by 0.5_5 eV from E_F. This characterizes a rather pronounced pseudo-gap in the decagonal quasicrystal. Note that,

although E_F in the calculation is not exactly at a minimum of the curves, our experimental data for Al states and the calculation by Trambly de Laissardière and Fujiwara (1994a, b) are in good agreement.

In this calculation, Cu atoms are in two different kinds of cluster (large and small) and there are also two different Co sites in the large clusters. The maximum of the Cu d states are at 3.5 eV from E_F and 4.35 eV from E_F in the large and small clusters, respectively. In the same way, the DOS maxima corresponding to the two different Co sites in the large clusters are at 1.74 eV and 2.72 eV, respectively. The experimental results show that Cu states are at 3.9 eV from E_F, which suggests that, in the sample used, whose Cu nominal concentration is lower than that of the model alloy, the Cu atoms should be located mainly in large clusters according to Burkov's model. A discrepancy remains as far as Co atoms are concerned since none of the positions as deduced from the model provide spectral distributions in agreement with the experimental results.

Recently, using the tight-binding LMTO basis and the recursion method, Sabiryanov *et al* (1995) have studied the electronic structure of decagonal and crystalline Al–Cu–Co alloys also based on the structural model proposed by Burkov (1991, 1992). Comparison between the calculated partial Al, Cu and Co DOSs and our experimental results shows no agreement for the position of spectral features or for intensity at E_F. Note, however, that no partial DOS calculation is shown for clusters with a Cu content lower than the Co content, which is the case in the experimental sample. Sabiryanov *et al* (1995) conclude that a local minimum in the DOS at E_F is exhibited only by clusters with a Cu concentration higher than the Co concentration; no minimum in the total DOS distribution at E_F is observed for clusters with equal or almost equal Cu and Co concentrations. To establish their results, these workers argue that the XPS investigation by Stadnik *et al* (1995a, b) of the OB states of $Al_{65}Cu_{20}Co_{15}$ did not provide evidence of a pseudo-gap at E_F. Let us recall here that, because of the photoemission cross sections that noticeably favour d states with respect to sp states, the XPS technique cannot provide a clear view of the s- and p-state distributions. Note also that the Al DOSs calculated by Sabiryanov *et al* (1995) disagree with those calculated by Trambly de Laissardière and Fujiwara (1994a, b) although both calculations are made for a Cu nominal concentration higher than the Co concentration.

As mentioned above, Stadnik *et al* (1995a, b) have investigated OB states using XPS measurements. These provide essentially the Co and Cu state distributions spatially averaged within a small depth of the sample and a superficial layer whose contribution may be significant. These workers do not report *in situ* chracterization of the surface of the sample that they measure. The XPS curve exhibits two well separated broad peaks 0.7 and 3.7 eV below E_F. Our SXS measurements of the energy positions of the Cu and Co 3d states agree with the XPS data.

We can now discuss our results for $Al_{70}Co_{15}Ni_{15}$. Because there are no calculations for this system, we shall compare with calculations (tight binding and LMTO ASA) as well as with experimental results for crystalline Al_5Co_2 (Pêcheur *et al* 1995). Indeed this latter alloy is an approximant of quasicrystalline decagonal phases (Song and Ryba 1992). We have shown experimentally and theoretically (Pêcheur *et al* 1995) that the TM 3d states in Al_5Co_2 (Co 3d states) are present about 1.5 eV below E_F and interact with Al hybridized p–d states, whereas far from E_F, below about 4 eV, the Al states are essentially s like (figure 10). The same should hold true for $Al_{70}Co_{15}Ni_{15}$. Indeed, the shapes of the Al 3p and Al 3s, d curves in the quasicrystal and in the approximant are somewhat related. The main differences lie in the facts that firstly for $Al_{70}Co_{15}Ni_{15}$ just after the edge the Al 3p curve is more structured than for Al_5Co_2 owing to the interaction with two different TMs in the quasicrystal which occur at slightly different binding energies and secondly the intensity

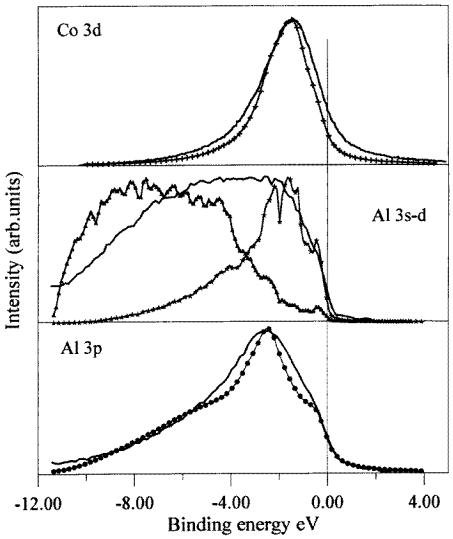

Figure 10. Calculated and experimental electronic distributions for crystalline Al_5Co_2. Experimental curves: ——. Calculated curves: —|— Co 3d, —●— Al 3p, —▲— Al 3s, —×— Al 3d. The calculated curves were obtained from the theroetical partial densities of states of Pêcheur *et al* (1996) broadened by a Lorentzian distribution to account for the width of the inner level involved in the x-ray transitions.

of the Al 3s, d curve for $Al_{70}Co_{15}Ni_{15}$ is less important within an energy range of about 3 eV below E_F than for Al_5Co_2. We ascribe these variations to differences in the strength of interactions between Al and TM elements in both alloys. Note that, for $Al_{70}Co_{15}Ni_{15}$, almost pure p-like states should be present around 2 and 3 eV below E_F because of the presence of feature b corresponding to a relative minimum β of the Al 3s, d curve and because of the plateau in the 3 eV energy range just before feature γ of the Al 3s, d curve which coincides with the maximum c of the Al 3p curve.

Compared with pure FCC Al, in the $Al_{70}Co_{15}Ni_{15}$ quasicrystal, the edges of the Al subbands are pushed significantly away from E_F to the centre of the OB. The Al 3p intensity at E_F is about 17% of the maximum intensity and the half-maximum intensity is distant from E_F by 0.6 ± 0.1 eV. Thus a rather pronounced pseudo-gap is observed in the Al state distribution of this decagonal quasicrystal. This has not been observed by Stadnik *et al* (1995(a) (b)) from XPS measurements on a decagonal quasirystal of the same composition. Let us recall again that, owing to the photoionization cross section, these workers cannot obtain any information concerning Al states at the energies where these overlap MT states.

Note that the shapes of the spectral distributions as well as the observation of a pseudo-gap at the Fermi level in the Al distributions in the Al–Cu–Co and Al–Ni–Co alloys are in agreement with previous results from the SXS experiments that we performed on other Al–Cu–TM (Belin *et al* 1992) and Al–TM decagonal phases (Belin and Traverse 1991, Belin *et al* 1991).

The shapes of the distribution curves of Cu and TM 3d states in both $Al_{65}Cu_{15}Co_{20}$ and $Al_{70}Co_{15}Ni_{15}$ quasicrystals are not affected by the alloying as expected and already observed in other alloys for d-like states (Belin and Traverse 1991, Belin *et al* 1991, 1992). For $Al_{70}Co_{15}Ni_{15}$, the curve for unoccupied Ni d–s states no longer preserves a localized-like (non-extended-like) character in the samples. Indeed, as pointed out in the previous section,

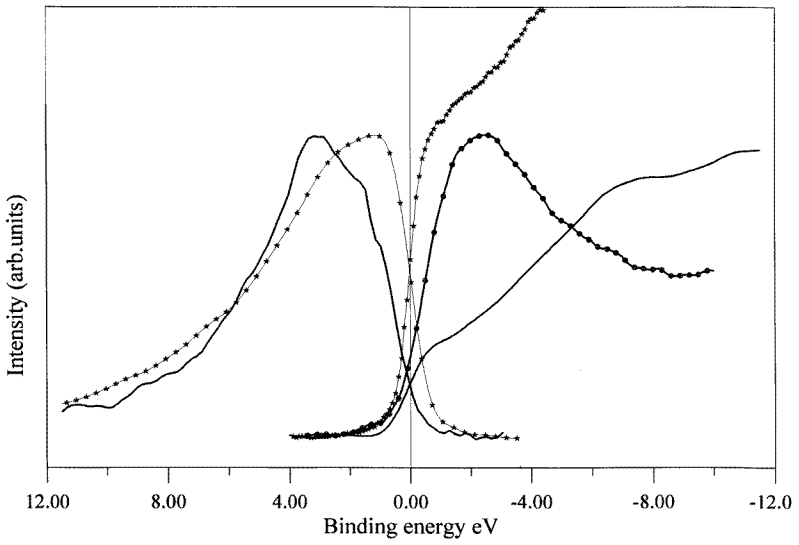

Figure 11. Al 3p (left side) and Al p (right side) distribution curves for pure Al (——★——) and for $Al_{70}Co_{15}Ni_{15}$ (——) as adjusted to the same intensity at the Fermi level. The unoccupied Ni s–d distribution curve is also plotted, adjusted to its maximum intensity.

the unoccupied states are mainly s–d in character with no clear pure d-like contribution. This could be due to filling of Ni d orbitals following charge transfer originating from Al atoms in the alloy. The shift of the Cu $2p_{3/2}$ levels towards the position of oxides may also indicate that some d-like character could be expected for the unoccupied distributions of this element in $Al_{65}Cu_{15}Co_{20}$; charge transfer from Cu atoms could be anticipated in $Al_{65}Cu_{15}Co_{20}$. The result of all these charge transfers may induce some covalent bonding in the quasicrystalline alloys in which they happen. More enlightenment is expected from the investigation of Co and Cu unoccupied states that is in progress and will be reported elsewhere compared with an Al–Cu–Co crystalline approximant.

Figure 11 displays the Al p distribution curves for pure Al and for $Al_{70}Co_{15}Ni_{15}$ as adjusted to the intensity of the Al 3p curve at E_F. This adjustment shows that, although all Al sites of the alloy are probed together, there is a noticeable depletion in both OB and UB Al p-like states in the vicinity of the Fermi level; this is less important than it is in icosahedral quasicrystals of high resistivity (Belin-Ferré and Dubois 1996). The unoccupied Ni s–d distribution curve is also plotted in this figure. From the overlap between the distribution curves of unoccupied states, it is confirmed that the first conduction states averaged over the bulk material should be of extended character.

Along the quasiperiodic planes, for $Al_{70}Co_{15}Ni_{15}$ the resistivity at 4 K has been measured to be 255 ± 20 $\mu\Omega$ cm whereas it is about 100 $\mu\Omega$ cm along the periodic direction (Gozlan 1991). This demonstrates the strong anisotropy of the material which cannot be distinguished by either the SXS or the XPS experiments undertaken so far. The resistivity value in the quasiperiodic direction is, however, not as high as those measured for other ternary icosahedral quasicrystals. In the highly resistive quasicrystals, we assumed that the extreme high resistivities were due to both important depletion of unoccupied Al extended states and the presence near E_F of a few unoccupied localized d-like states. For $Al_{70}Co_{15}Ni_{15}$, it looks like no such localized states exist near E_F that could somewhat prevent the motion of

electrons throughout conduction states. However, we observe that the depletion of Al states in the vicinity of E_F is more important than in Hume-Rothery phases such as Al_2Cu (Dong *et al* 1994) or Al_7Cu_2Fe (Belin *et al* 1994) which is consistent with the higher resistivity of this alloy with respect to the usual Al-based intermetallics. This might indicate that the experimental results reported here, although spatially averaged, could involve a significant contribution from the quasiperiodic planes of the sample. In the case of $Al_{66}Cu_{30}Co_{14}$, Trambly de Laissardière and Fujiwara (1994a, b) have calculated the dispersion curves in the periodic and non-periodic directions. These workers pointed out that, in the quasiperiodic directions, the curves are much more dispersionless than in the periodic direction and are similar to those found in the two-dimensional Penrose lattice. In the two-dimensional case, the dispersionless curves lead to very spiky DOSs the investigation of which by experimental means is quite a challenge since it would require energy resolutions less than a millielectronvolt. We have suggested above that a slight covalent-like character of bonding could be due to a small charge transfer from Al atoms. Such a covalency could also be invoked to explain the resistivity of the sample. This has to be confirmed by the study of Co empty states in this alloy as well as by that of the unoccupied states in $Al_{65}Cu_{15}Co_{20}$.

5. Conclusion

In this paper we have presented the results of an experimental investigation of partial occupied and unoccupied electronic distributions in two different decagonal quasicrystals, namely $Al_{65}Cu_{15}Co_{20}$ and $Al_{70}Co_{15}Ni_{15}$. For $Al_{65}Cu_{15}Co_{20}$, we have shown that, in the OB, the Al states are p–d hybridized and interact with Co 3d states in the vicinity of E_F and that they are mainly s like in character beyond 5 eV from E_F. The Cu 3d states are found in the middle of the OB; their interaction with the Al states produces a depletion of the Al 3s–d distribution curve and a shoulder in the Al 3p curve. A noticeable pseudo-gap is shown at E_F in the Al electronic distributions. For $Al_{70}Co_{15}Ni_{15}$, a pseudo-gap at E_F in the Al distributions is also shown. The interaction between Al states and Co and Ni 3d states gives rise to distinct shoulders on the Al distribution curves in the vicinity of E_F. The OB Al states are p–d hybridized over the first electronvolt beyond E_F and are almost pure s like below 5 eV from E_F. In the UB, we have shown that the Al p states overlap Ni s–d states, which suggest a charge transfer from Al to Ni. Although the information which is obtained by our experimental techniques is spatially averaged over the bulk material and does not in principle clearly distinguish between quasiperiodic and periodic contributions, we suggest that, in $Al_{70}Co_{15}Ni_{15}$, information about the Al p UB presumably may be ascribed to a significant contribution from the quasiperiodic planes.

For $Al_{65}Cu_{15}Co_{20}$, our results for the Al and Cu OBs are in good agreement with a calculation by Trambly de Laissardière and Fujiwara (1994a, b) based on the model proposed by Burkov (1991, 1992). For $Al_{70}Co_{15}Ni_{15}$, our data agree fairly well with previous results obtained by theoretical and experimental means on the crystalline approximant Al_5Co_2. The present results are in line with previous measurements using the same methodology on other quasicrystalline alloys of icosahedral or decagonal atomic structure.

Acknowledgments

We acknowledge G Trambly de Laissardière and T Fujiwara for kindly supplying figure 9. We thank A M Flank and P Lagarde for assistance during the measurements at LURE. This work has been in part supported by the Austrian Ministry of Research East West Co-operation under the title ‘Soft X-ray Emission Spectroscopy of Metallic Systems’.

References

Belin E and Traverse A 1991 *J. Phys.: Condens. Matter* **3** 2157
Belin E and Dankházi Z 1993 *J. Non-Cryst. Solids* **153–4** 298
Belin E, Dankházi Z, Sadoc A, Calvayrac Y, Klein T and Dubois J M 1992 *J. Phys.: Condens. Matter* **4** 4459
Belin E, Dankházi Z, Sadoc A and Dubois J M 1994a *J. Phys.: Condens. Matter* **6** 8771
Belin E, Dankházi Z, Sadoc A, Dubois J M and Calvayrac Y 1994b *Europhys. Lett.* **26** 677
Belin E, Dankházi Z, Sadoc A, Flank A-M, Poon J, Müller H and Kirchmayr H 1995 *Proc. 5th Int. Conf. on Quasicrystals* ed C Janot and R Mosseri (Singapore: World Scientific) p 435
Belin E, Kojnok J, Sadoc A, Traverse A, Harmelin M, Berger C and Dubois J M 1991 *J. Phys.: Condens. Matter* **4** 1057
Belin-Ferré E and Dubois J M 1996 *J. Phys.: Condens. Matter* submitted
Bendersky L A 1985 *Phys. Rev. Lett.* **55** 1426
Berger C, Belin E and Mayou D 1993 *Ann. Chim. Fr.* **18** 485
Burkov S E 1991 *Phys. Rev. Lett.* **67** 614
——1992 *J. Physique* **2** 695
Dankházi Z, Trambly de Laissardiere G, Nguyen Manh D, Belin E and Mayou D 1993 *J. Phys.: Condens. Matter* **5** 3339
Dong C, Perrot A, Dubois J M and Belin E 1994 *Mater. Sci. Forum* **150–1** 403
Fettweiss M, Launois P, Dénoyer F, Reich R and Lambert M 1994 *Phys. Rev.* B **49** 15 573
Fuggle J C, Källne, Watson L M and Fabian D J 1977 *Phys. Rev.* **16** 750
Gozlan A 1991 *PhD Thesis* University of Grenoble
He J X, Wu Y K and Kuo K H 1988 *J. Mater. Sci. Lett.* B **7** 1284
Krause M O and Oliver J H 1979 *J. Phys. Chem. Ref. Data* **8** 329
Léonard P 1978 *J. Phys. F: Met. Phys.* **8** 467
Liao X Z, Kuo K H, Zhang H and Urban K 1992 *Phil. Mag.* B **66** 549
McRae E G, Malic R A, Lalonde T H, Thiel F A, Chen H S and Kortan A R 1990 *Phys. Rev. Lett.* **65** 883
Nakamua Y and Mizutani U 1994 *Mater. Sci. Eng.* A **181–2** 790
Nozières P and de Dominicis C T 1969 *Phys. Rev.* **178** 6105
Papaconstantopoulos D A 1986 *Handbook of the Band Structures of Elemental Solids* (New York: Plenum) pp 208 (Al), 122 (Cu), 114, 118 (Ni), 105, 109 (Co)
Pêcheur P, Belin E, Toussaint G, Trambly de Laissardière G, Mayou D, Dankházi Z, Muller H and Kirchmayr H 1995 *Proc. 5th Int. Conf. Quasicrystals* ed C Janot and R Mosseri (Singapore: World Scientific) p 501
Poon S J 1992 *Adv. Phys.* **41** 303
Sabiryanov R F, Bose S K and Burkov S E 1995 *J. Phys.: Condens. Matter* **7** 5437
Sadoc A, Belin E, Dankházi Z and Flank A M 1993 *J. Non-Cryst. Solids* **153–154** 338
Schechtman D, Blech I, Gratias D and Cahn J W 1984 *Phys. Rev. Lett.* **53** 1951
Song S and Ryba E R 1992 *Phil. Mag. Lett.* **65** 85
Stadnik Z M, Zhang G W, Tsai A P and Inoue A 1995a *Phys. Rev.* B **51** 11 358
——1995b *Phys. Lett.* **237A**
Steurer W 1993 *J. Non-Cryst. Solids* **154–5** 92
Steurer W 1994 *Mater. Sci. Forum* **150–1** 15
Steurer W, Haibach T, Zhang B, Kek S and Luck R 1993 *Acta Crystallogr* B **49** 661
Takeuchi S and Kimura K 1987 *J. Phys. Soc. Japan* **56** 982
Trambly de Laissardière G and Fujiwara T 1994a *Mater. Sci. Eng.* A **179–80** 722
——1994b *Phys. Rev.* B **50** 9843
Traverse A, Belin-Ferre E, Dankházi Z, Mendoza-Zelis L, Laborde O and Porter R 1996 *J. Phys.: Condens. Matter* **8** 3843
Tsai A P, Inoue A and Masumoto T 1989 *Mater. Trans.* **30** 300, 436
Wittmann R, Fettweiss M, Launois P, Reich R and Dénoyer F 1995 *Phil. Mag. Lett.* **71** 147
Yeh J J 1993 *Atomic Calculation of Photoionization Cross Sections and Asymmetry Parameters* (New York: Gordon and Breach)